Soft-core binary fluid exhibiting a λ-line and freezing to a highly delocalized crystal

2004 J. Phys.: Condens. Matter 16 L297

(http://iopscience.iop.org/0953-8984/16/23/L03)

INSTITUTE OF PHYSICS PUBLISHING JOURNAL OF PHYSICS: CONDENSED MATTER

J. Phys.: Condens. Matter **16** (2004) L297–L303 PII: S0953-8984(04)79996-8

LETTER TO THE EDITOR

Soft-core binary fluid exhibiting a λ-line and freezing to a highly delocalized crystal

A J Archer[1,2], C N Likos[2,1] and R Evans[1]

[1] H H Wills Physics Laboratory, University of Bristol, Bristol BS8 1TL, UK
[2] Institut für Theoretische Physik II, Heinrich-Heine-Universität Düsseldorf, Universitätsstraße 1, D-40225 Düsseldorf, Germany

Received 29 April 2004
Published 28 May 2004
Online at stacks.iop.org/JPhysCM/16/L297
DOI: 10.1088/0953-8984/16/23/L03

Abstract

We show that a simple soft-core binary fluid mixture with purely repulsive interactions exhibits a λ-line, i.e., a line of continuous transitions to a state characterized by undamped periodic concentration fluctuations (microphase separation). For states in the disordered fluid phase the bulk pair correlation functions exhibit strong 1–2 ordering, similar to that found in ionic fluids, which is also reflected in the density profiles of confined fluids. The latter display fluid layers alternating from rich in species 1 to rich in species 2. We argue that the λ-instability drives a freezing transition to a highly delocalized crystal, with Lindemann ratios that can exceed 90% near melting.

Soft matter systems are complex, multicomponent mixtures. They commonly consist of macromolecular entities in a microscopic solvent and include a number of additional constituents. The enormous flexibility in controlling the architecture of the macromolecules, the solvent type and the composition of the mixture bring about a concomitant freedom in tailoring the effective interaction potentials between the dissolved mesoscopic particles [1]. Recently much attention has been devoted to the derivation of such effective interactions for polymeric entities in solution. Important examples are linear [2] and star polymers [3] as well as dendrimers [4]. Often, the centre of mass of the fractal polymer is chosen as an effective coordinate. In this case, and in contrast to the interaction potentials commonly known from the realm of atomic systems, effective interactions can be ultrasoft and bounded, i.e., free of divergence even for full overlap between the centres of mass. This fact has rekindled interest in the study of the properties of systems interacting by means of such potentials, a prominent example being the Gaussian core model (GCM), first introduced by Stillinger [5]. The phase behaviour of the one-component GCM is rich, displaying crystallization and 'inverted melting' at sufficiently low temperatures [6]. Even richer is the structural and phase behaviour of binary Gaussian mixtures, which can exhibit fluid–fluid demixing and a wealth of interesting wetting properties when brought into contact with repulsive walls [7]. In this letter, we focus on a binary GCM fluid that does not display fluid–fluid demixing. Rather, the present mixture

displays what is often termed a λ-transition in the ionic fluid literature[3] or, more generally, *microphase* separation, i.e., an instability with respect to periodic density modulations [9].

A very reliable density functional theory (DFT) approach has been developed for the GCM [6]. Within the realm of this DFT, we investigate the structure of the homogeneous fluid and also locate the freezing and λ-transitions of the system. Our model is specified by the pair potentials between particle species i and j: $v_{ij}(r) = \epsilon_{ij}\exp(-r^2/R_{ij}^2)$, where $\epsilon_{ij} > 0$ denotes the energy and R_{ij} determines the range of the ij interaction; $1 \leqslant i, j \leqslant 2$. Provided $\epsilon_{ii} \simeq 2k_{\mathrm{B}}T$, then the GCM can be thought of as a simple model for polymers in a good solvent, where the Gaussian potential represents the effective potential between the centres of mass of a pair of polymers [1]. In this case R_{ii} is approximately the radius of gyration for polymer species i. At such reduced temperatures the one-component GCM is fluid at all densities [1, 6]. For an athermal binary mixture of polymers one expects, based on simulation results [10], that the parameters for the effective pair potential between unlike species are given by the mixing rules: $\epsilon_{12} \lesssim \epsilon_{11} = \epsilon_{22}$ and $R_{12}^2 = (R_{11}^2 + R_{22}^2)/2$ [2, 7, 10], i.e. $R_{12} = (1+\Delta)(R_{11} + R_{22})/2$, where the non-additivity parameter $\Delta > 0$. This positive non-additivity can drive a demixing transition if the density of the fluid is sufficiently high [2, 7]. However, in the present study we are interested in the case where $\Delta < 0$, i.e., negative non-additivity. In this case the binary fluid does not demix. Physically, the nonadditivity can be tuned by appropriate chemistry in polymer mixtures or by modifications of the macromolecule architecture in dendrimer mixtures, which are also described by Gaussian interactions [4]. The pair potential parameters we choose are $\epsilon_{11} = \epsilon_{22} = 2\,k_{\mathrm{B}}T$, $\epsilon_{12} = 1.8877\,k_{\mathrm{B}}T$, $R_{22} = 0.665R_{11}$ and $R_{12} = 0.6R_{11}$. Apart from this choice of value for R_{12}, these parameters are the same as those used for much of the work in [7] (where $R_{12} = 0.85R_{11}$ was used).

We employ the simple random-phase approximation (RPA) for the excess Helmholtz free energy functional of the inhomogeneous mixture:

$$\mathcal{F}_{\mathrm{ex}}[\{\rho_i\}] = \tfrac{1}{2}\sum_{ij}\int \mathrm{d}\mathbf{r}_1 \int \mathrm{d}\mathbf{r}_2\, \rho_i(\mathbf{r}_1)\rho_j(\mathbf{r}_2)v_{ij}(|\mathbf{r}_1 - \mathbf{r}_2|), \tag{1}$$

where $\rho_i(\mathbf{r})$ is the one-body density profile for species i. This functional, which generates the RPA for the pair direct correlation functions, $c_{ij}^{(2)}(\mathbf{r}_1, \mathbf{r}_2) = -\beta\delta^2\mathcal{F}_{\mathrm{ex}}/\delta\rho_i\delta\rho_j = -\beta v_{ij}(|\mathbf{r}_1 - \mathbf{r}_2|)$, where $\beta = (k_{\mathrm{B}}T)^{-1}$ [11], is surprisingly accurate for calculating the bulk fluid structure and thermodynamics of the GCM, provided the fluid density is sufficiently high, so that the soft cores of the GCM particles overlap strongly [1]. In figure 1 we display the radial distribution functions $g_{ij}(r)$, calculated for a fluid with total density $\rho R_{11}^3 = 5$ and concentration of species 2, $x \equiv \rho_2^{\mathrm{b}}/\rho = 0.4$ (ρ_i^{b} is the bulk density of species i). These are obtained from Monte Carlo (MC) simulations and from the DFT via the test-particle route. Within DFT, the profiles $\rho_i(\mathbf{r})$ are calculated by minimizing the grand potential functional [11, 7]:

$$\Omega[\{\rho_i\}] = \mathcal{F}[\{\rho_i\}] - \sum_{i=1}^{2}\int \mathrm{d}\mathbf{r}\,(\mu_i - V_i(\mathbf{r}))\rho_i(\mathbf{r}), \tag{2}$$

where $\mathcal{F} = \mathcal{F}_{\mathrm{id}} + \mathcal{F}_{\mathrm{ex}}$ and $\mathcal{F}_{\mathrm{id}}$ is the ideal gas part of the free energy functional, μ_i are the chemical potentials and $V_i(\mathbf{r})$ are the external potentials, in this case those due to the fixed test particle of species j. Then, $g_{ji}(r) = \rho_i(r)/\rho_i^{\mathrm{b}}$. In general, we find that the RPA test-particle results for $g_{ij}(r)$ are more accurate than those obtained using the RPA closure for $c_{ij}^{(2)}(r)$ in the bulk Ornstein–Zernike (OZ) equations. They are also very close to those from the HNC

[3] See e.g. Stell [8]. The λ-line refers to a line of continuous transitions (analogous to Néel points in spin 1 Ising antiferromagnets) from a charge-disordered state to a periodic charge-ordered state where the charge–charge correlation function $rh_{qq}(r)$ is purely oscillatory. For a recent discussion of charge correlations near a λ-line see Ciach *et al* [8].

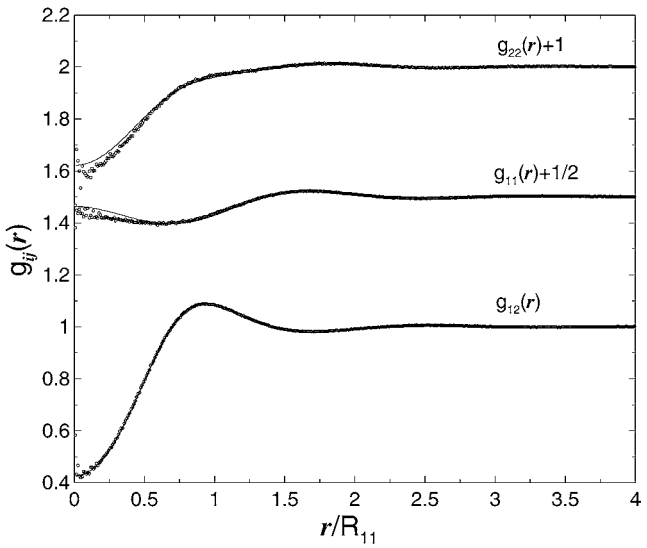

Figure 1. Radial distribution functions $g_{ij}(r)$ for a binary GCM mixture with total density $\rho R_{11}^3 = 5$ and concentration $x = \rho_2^b/\rho = 0.4$. The open circles denote the MC-simulation results and the solid curves the DFT test-particle results.

closure to the OZ equations [12, 1, 2, 7]. From figure 1 we see that the RPA functional (1) provides a very accurate account of the correlations at this particular state point and this leads us to consider higher total densities ρ where the RPA should be even more reliable. Here we find more pronounced ordering.

On increasing ρ, the $g_{ij}(r)$ display a growing tendency for the fluid to order with the particles of species 1 preferring species 2 as nearest neighbours and vice versa. We refer to this as 1–2 ordering; it is similar to what occurs in a charged fluid where cations prefer to be surrounded by anions [12] and is illustrated in figure 2 where we plot the concentration–concentration correlation function $h_{cc}(r) = (1-x)^2 h_{11}(r) + x^2 h_{22}(r) - 2x(1-x)h_{12}(r)$, and the number–number correlation function $h_{nn}(r) = (1-x)^2 h_{11}(r) + x^2 h_{22}(r) + 2x(1-x)h_{12}(r)$ calculated at the state point with density $\rho R_{11}^3 = 12$ and concentration $x = 0.15$; $h_{ij}(r) = g_{ij}(r) - 1$. There are pronounced oscillations in $h_{cc}(r)$, showing the tendency of the fluid to exhibit 1–2 ordering. The function $h_{nn}(r)$ is relatively flat, i.e., the number–number correlations are much weaker. In the inset to figure 2 we plot the structure factor $S_{11}(k)$ on path A in the phase diagram (see figure 3). We see the development of a pronounced peak in $S_{11}(k)$ at $k = k_c \simeq \pi/R_{12}$, whose height increases continuously and eventually diverges as the concentration x increases towards a certain value x_λ at fixed $\rho R_{11}^3 = 12$. The other two structure factors, $S_{12}(k)$ and $S_{22}(k)$, also diverge at the same point, and the three pair correlation functions become purely oscillatory for large r: $rh_{ij}(r) \sim A_{ij}^c \cos(k_c r + \theta_{ij})$, $i, j = 1, 2$, as $x \to x_\lambda$. We recall that the partial structure factors are defined as $S_{ij}(k) = \delta_{ij} + \sqrt{\rho_i^b \rho_j^b}\hat{h}_{ij}(k)$, where $\hat{h}_{ij}(k)$ are the Fourier transforms of $h_{ij}(r)$. In Fourier space, the OZ equations for $h_{ij}(r)$ can be written as [12] $\hat{h}_{ij}(k) = N_{ij}(k)/D(k)$, where $N_{ij}(k) = \hat{c}_{ij}(k) + \delta_{ij}\rho_i^b[\hat{c}_{12}^2(k) - \hat{c}_{12}(k)\hat{c}_{22}(k)]$ and

$$D(k) = [1 - \rho_1^b \hat{c}_{11}(k)][1 - \rho_2^b \hat{c}_{22}(k)] - \rho_1^b \rho_2^b \hat{c}_{12}^2(k). \tag{3}$$

The $\hat{c}_{ij}(k)$ are the Fourier transforms of $c_{ij}^{(2)}(r)$. If in certain domains of the phase diagram $D(k) = 0$ for $k = k_c \neq 0$, then the partial structure factors diverge at some (real) wavenumber

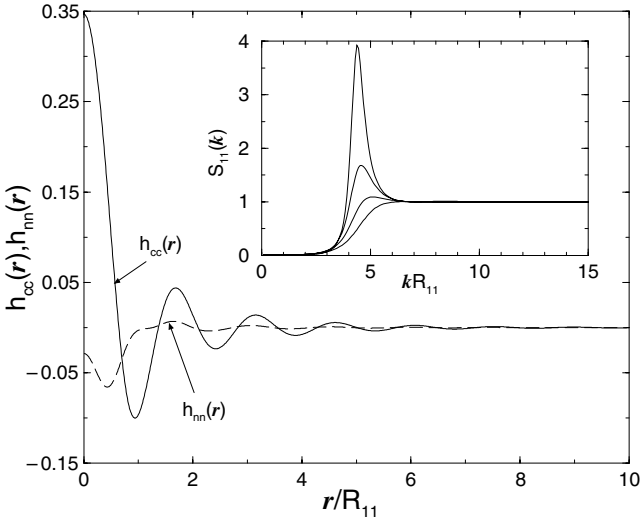

Figure 2. The correlation functions $h_{cc}(r)$ and $h_{nn}(r)$ calculated using the DFT test particle route, for the binary GCM fluid with total density $\rho R_{11}^3 = 12$ and $x = 0.15$. In the inset the partial structure factor $S_{11}(k)$ is plotted at concentrations $x = 0.0$, 0.05, 0.1 and 0.15 along path A in figure 3, at fixed $\rho R_{11}^3 = 12$. As x is increased further the height of the peak in $S_{11}(k)$ grows continuously, diverging at the λ-line.

k_c. Standard asymptotic analysis shows that in real space this corresponds to $rh_{ij}(r)$ having a purely oscillatory form as $r \to \infty$. We define the λ-line as the locus of points in the phase diagram at which $D(k_c) = 0$ (see footnote 3). Outside this line $D(k) > 0$ for all k values. We calculated the λ-line, plotted in figure 3, by determining the zeros of $D(k)$ in equation (3) within the RPA: $\hat{c}_{ij}(k) = -\beta\hat{v}_{ij}(k)$, where $\hat{v}_{ij}(k)$ are the Fourier transforms of the pair potentials $v_{ij}(r)$.[4] On the λ-line the fluid becomes unstable with respect to periodic concentration fluctuations with wavenumber $k_c \sim \pi/R_{12}$. The physical origin for this instability lies in the choice $R_{12} < R_{22} < R_{11}$; there is a lower potential energy for a particle to be located at a distance $\sim R_{12}$ from a particle of the opposite species, thereby generating 1–2 ordering. This is quite distinct from the recently found microphase separation in a *lattice model* [13], which is caused rather by the selection of the energetic prefactors ϵ_{ij} in $v_{ij}(r)$.

The occurrence of an instability of a fluid to periodic concentration modulations often signals the presence of a nearby freezing transition [14]. In order to investigate freezing, we used the simple RPA free energy functional, equation (1), to calculate both the fluid and the crystal free energies. In the case of the fluid, $\rho_i(\mathbf{r}) = \rho_i^b$ and the bulk Helmholtz free energy is very simple [2, 7]. For the crystal, we assume that the one-body density profiles have the following form:

$$\rho_i(\mathbf{r}) = \sum_n \eta_i \left(\frac{\alpha_i}{\pi}\right)^{3/2} \exp(-\alpha_i|\mathbf{r} - \mathbf{R}_n|^2), \tag{4}$$

$i = 1, 2$, i.e., a set of Gaussian density peaks, centred on a set of lattice sites located at $\mathbf{R}_n$. The parameters $\alpha_i^{-1/2}$ and η_i are the width and lattice site occupation numbers for each species. The latter are very important for bounded interactions, since multiple site occupancies are now allowed [15]. Given the occurrence of the λ-line, indicating the strong propensity of particles to favour the opposite species as nearest neighbours, we expect the crystal structure

[4] One can show that the test-particle and OZ routes yield the same poles of $\hat{h}_{ij}(k)$.

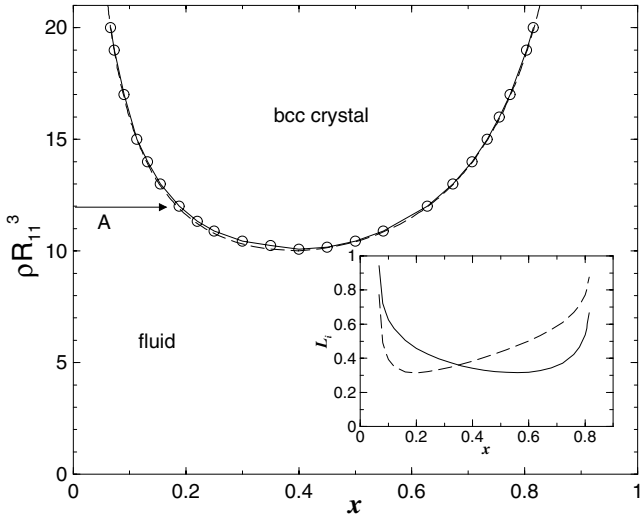

Figure 3. Phase diagram for the binary mixture of GCM particles determined by DFT. ρ is the total density and x is the concentration of the smaller species 2. The open circles joined by a solid curve denote the crystal–liquid phase boundary, and the dashed curve denotes the λ-line (see text). In the inset we plot the Lindemann ratios L_i for the crystal, calculated at constant density $\rho R_{11}^3 = 20$. The solid curve corresponds to L_1 (the larger species), and the dashed curve to L_2.

to reflect this 1–2 ordering. On this basis we chose as our trial crystal structure the bcc lattice, with one species centred on the unit cell corner, and the other species centred on the site at the centre of the unit cell, i.e., the CsCl crystal structure[5]. For a given density ρ and concentration x, the Helmholtz free energy functional for the crystal becomes a function, $\tilde{F}_c$, of α_1, α_2 and a, where a is the lattice constant. In order to calculate the free energy of the crystal we minimize $\tilde{F}_c(\alpha_1, \alpha_2, a)$ with respect to α_1, α_2 and a. From the resulting Helmholtz free energy per particle, f_c, we can calculate the pressure in the crystal, P, and the Gibbs free energy, $g_c(x, P) = f_c + P/\rho$. In order to determine the equilibrium phase, we calculate $g_c(x, P)$ along an isobar and compare this with the liquid state Gibbs free energy $g_l(x, P)$, along the same isobar. The coexisting solid and liquid densities are obtained by performing the common-tangent construction between the curves $g_c(x, P)$ and $g_l(x, P)$ [7]. We find that the difference in density, $\Delta\rho$, between the coexisting crystal and liquid is very small, typically $\Delta\rho/\rho < 0.1\%$ for points on the coexistence curve.

The full crystal–fluid phase boundary is plotted in figure 3. Since the density difference between the coexisting crystal and liquid is very small, we merely display the locus $g_c = g_l$ and omit the very narrow coexistence regions. The crystal–liquid phase boundary lies just inside the λ-line. We might, perhaps, have expected the former to lie outside the λ-line, i.e. crystallization might be expected to pre-empt the onset of an instability to periodic ordering, and we speculate that since the two are so close the crystal–liquid boundary might lie outside the λ-line in a more accurate theory. We have not calculated the free energy for any other lattice structures (see footnote 5). For a binary mixture of particles there are many potential lattice structures; however, the fact that the bcc lattice has a lower free energy than the liquid suggests that the system should be crystalline in some portions of the phase diagram. The occurrence of other

[5] We prefer the CsCl to the NaCl crystal structure since in the former the cation has eight neighbours as opposed to six. For the present GCM we therefore expect the CsCl structure to have a lower free energy than the NaCl structure.

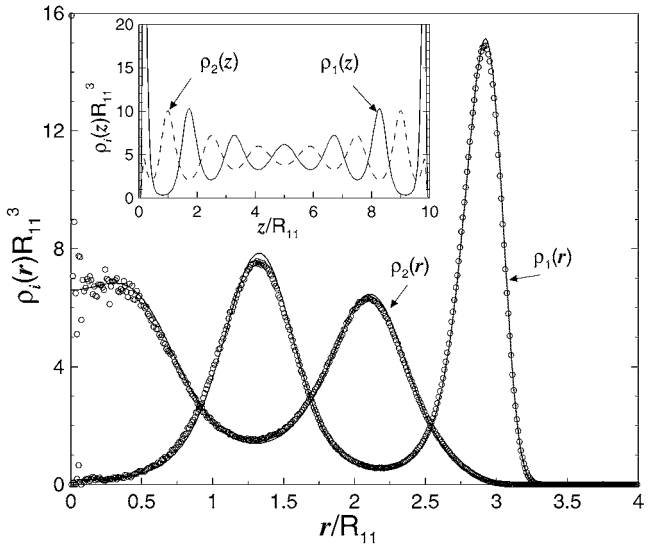

Figure 4. Fluid density profiles ρ_i for the binary GCM in a spherical cavity calculated for $N_1 = 700$ and $N_2 = 300$. The solid curves refer to the DFT results and the circles to those of Brownian dynamics simulations. In the inset we show the DFT profiles for the fluid confined in a planar slit of width $d = 10R_{11}$. For a specification of the wall–particle potentials, see the text.

ordered phases, such as 'lamellar-like' ones, which may intervene between the disordered fluid and the crystal, cannot be excluded, but we have not considered such phases in this work.

The most striking feature of the crystalline phase is that there are multiple occupancies on each lattice site[6], i.e., $\eta_i \geqslant 12$, and the particles on each lattice site are highly delocalized. This can be seen in the inset to figure 3, where we plot the Lindemann ratios, $L_i = \sqrt{2}/a\sqrt{\alpha_i}$, $i = 1, 2$, which are defined as the root mean square displacement of a particle of species i divided by $b = a\sqrt{3}/2$, the nearest neighbour distance, calculated for constant $\rho R_{11}^3 = 20$. We find that near to crystal–liquid coexistence L_i can be as high as 90%; recall that a typical atomic crystal is known to melt when $L_i \simeq 10\%$. Clearly, the present crystal is highly delocalized. Another feature of the crystal is that the lattice constant varies very little, ranging from $a \simeq 1.35R_{11}$ to $1.5R_{11}$ in different parts of the phase diagram. On increasing the total density for a constant composition x, we find that a remains roughly constant and η_i increases, in close similarity to the case of a one-component system (in the ρ–T plane) whose bounded interparticle potential has a Fourier transform that displays oscillatory behaviour [15].

The presence of the λ-line also has very pronounced effects on *inhomogeneous* fluid density profiles. In figure 4 we display the profiles calculated for $N_1 = 700$ particles of species 1 and $N_2 = 300$ particles of species 2, in a spherical cavity with potentials $\beta V_i(r) = 10(r/3R_{11})^{10}$. The agreement between the DFT and simulation results is remarkably good; the DFT captures all the details of the highly structured profiles. Note that within the grand canonical DFT $\langle N_i \rangle$, the *mean* number of particles of species i in the cavity, is constrained. The corresponding chemical potentials μ_i can be associated with a bulk reservoir with $x = 0.477$ and $\rho R_{11}^3 = 6.7$—a state point well removed from the λ-line. When the fluid mixture is confined between two parallel walls, separated by the distance d and exerting potentials $\beta V_i(z) = \exp(-z/R_{11})/(z/R_{ii}) + \exp(-(d-z)/R_{11})/((d-z)/R_{ii})$, we find it

[6] For the one-component GCM crystal the lattice sites have single occupancy, see [6].

orders into well defined layers alternating from rich in species 1 to rich in species 2. In the inset to figure 4 we plot the density profiles for a slit with $d = 10R_{11}$; the chemical potentials correspond to a reservoir with $x = 0.5$ and $\rho R_{11}^3 = 9.5$, a state chosen to be close to the λ-line. The striking alternating layered structure of the fluid may prove to enhance its lubricating properties.

In this letter we have shown that for a simple soft-core model binary fluid, exhibiting 1–2 ordering, the presence of a λ-transition has a significant effect on correlations in the bulk fluid, even for states relatively far from the λ-transition. The latter drives a freezing transition to a highly delocalized solid and also manifests itself in the form of inhomogeneous fluid density profiles which show a confined fluid ordering into alternating layers of the two species. Although we have restricted our present study to the binary GCM, we expect the λ-line and the associated phenomena to occur quite generally for binary mixtures whose components interact by means of bounded potentials which display negative non-additivity.

We thank H Löwen for a critical reading of the manuscript. AJA acknowledges the support of EPSRC under grant number GR/S28631/01 and from the DFG through the SFB-TR6. CNL has been supported by the DFG through a Heisenberg Fellowship.

References

[1] Likos C N 2001 *Phys. Rep.* **348** 267
[2] Louis A A *et al* 2000 *Phys. Rev. Lett.* **85** 2522
Louis A A *et al* 2000 *Phys. Rev.* E **62** 7961
[3] Likos C N *et al* 1998 *Phys. Rev. Lett.* **80** 4450
[4] Likos C N *et al* 2002 *J. Chem. Phys.* **117** 1869
[5] Stillinger F H 1976 *J. Chem. Phys.* **65** 3968
[6] Lang A *et al* 2000 *J. Phys.: Condens. Matter* **12** 5087
[7] Archer A J and Evans R 2001 *Phys. Rev.* E **64** 041501
Archer A J and Evans R 2002 *J. Phys.: Condens. Matter* **14** 1131
Archer A J and Evans R 2003 *J. Chem. Phys.* **118** 9726
[8] Stell G 1995 *J. Stat. Phys.* **78** 197
Ciach A, Góźdź W T and Evans R 2003 *J. Chem. Phys.* **118** 3702
[9] Sear R P and Gelbart W M 1999 *J. Chem. Phys.* **110** 4582 and references therein
[10] Dautenhahn J and Hall C K 1994 *Macromolecules* **27** 5399
[11] Evans R 1992 *Fundamentals of Inhomogeneous Fluids* ed D Henderson (New York: Dekker) chapter 3
[12] Hansen J-P and McDonald I R 1986 *Theory of Simple Liquids* 2nd edn (London: Academic)
[13] Finken R *et al* 2004 *J. Phys. A: Math. Gen.* **37** 577
[14] This notion can be traced back to Kirkwood J G and Monroe E 1941 *J. Chem. Phys.* **9** 514, see also [15]
[15] Likos C N *et al* 2001 *Phys. Rev.* E **63** 031206